

IEEE copyright notice

Personal use of this material is permitted. However, permission to reprint/republish this material for advertising or promotional purposes or for creating new collective works for resale or redistribution to servers or lists, or to reuse any copyrighted component of this work in other works must be obtained from the IEEE. Contact: Manager, Copyrights and Permissions / IEEE Service Center / 445 Hoes Lane / P.O. Box 1331 / Piscataway, NJ 08855-1331, USA. Telephone: + Intl. 908-562-3966.

LOCAL AND GLOBAL CALIBRATION FOR HIGH-RESOLUTION DOA ESTIMATION IN AUTOMOTIVE RADAR

Michael Schoor and Bin Yang

Chair of System Theory and Signal Processing, Universität Stuttgart, Germany
{michael.schoor, bin.yang@Lss.uni-stuttgart.de}
www.LSS.uni-stuttgart.de

ABSTRACT

Calibration of an antenna array is very important for high-resolution direction-of-arrival (DOA) estimation. In this paper, we study this issue for an automotive frequency modulated continuous wave (FMCW) radar whose low-cost dielectric lens antenna causes, in addition to the coupling between sensor elements and gain or phase mismatch, direction-dependent perturbations to the sensor response. We apply both global and local calibration methods and compare their performance.

1. INTRODUCTION

Automotive radar sensors are used for many driver assistance and safety systems such as adaptive cruise control (ACC), lane change monitoring, brake assistant, collision warning, and prevention. In present automotive radar systems, only targets in different distance-velocity cells can be resolved. The increasing demand on safety requirements leads to efforts improving the DOA estimation to allow resolution of targets even in the same distance-velocity cell. This is one important goal of our KRAFAS project [1] (cost optimized radar sensor for active driver assistance systems).

Current automotive radar systems use the monopulse technique for DOA estimation, e.g. by comparing the received signal strength of several antenna beams [2]. The DOA resolution is poor since automotive radar have typically a low antenna aperture due to size and cost restriction. A natural solution is thus the use of well known high-resolution methods for DOA estimation, in particular the family of subspace based methods like MUSIC and ESPRIT [3] because they are relatively simple to implement. These methods, however, require a number of assumptions about the signal and antenna which are, unfortunately, not always satisfied in automotive applications. At least for the radar sensor we currently develop, we are facing a number of practical problems: a small number of snapshots, multipath propagation, targets overlapping in frequency domain due to FMCW, sometimes strongly correlated source signals, and sensor errors.

In this paper, we focus on the last issue. A low-cost dielectric lens of our radar sensor for focussing in elevation causes direction-dependent sensor response errors which have to be corrected

before high-resolution angle estimation. We report our experience with both global and local calibration methods [4, 5, 6, 7, 8].

The paper is organized as follows. Section 2 introduces our automotive radar antenna. Section 3 briefly reviews the concept of subspace based high-resolution DOA estimation. Local and global calibration of the antenna array are described in section 4 and compared in section 5 through computer experiments.

2. FMCW LONG RANGE AUTOMOTIVE RADAR

The automotive radar sensor under study is a long range radar based on (linear) FMCW modulation. Table 1 summaries its main specifications. The receiving antenna is a uniform linear array (ULA) consisting of $M = 8$ elements with an element spacing $d = \lambda$. This spacing leads to grating lobes, but also a narrow main lobe. It also allows for a better isolation between the elements reducing the cross coupling. Additionally, high-gain elements can be used to increase the signal-to-noise ratio (SNR) [9]. Since the transmitter antenna has a limited azimuth range as well, grating lobes do not cause serious problems.

frequency range [GHz]	76~77
distance range/accuracy/resolution [m]	2~200, 0.5, 2
velocity range/accuracy/resolution [m/s]	-60~20, 0.25, 1.1
azimuth range/accuracy/resolution [°]	-8~8, 0.4, 3

Table 1. Main specifications of the car radar sensor

Due to the FMCW modulation, the transmit frequency changes linearly in time within a ramp. The received signal exhibits a frequency difference called beat frequency. It is a linear function of both distance and Doppler shift of the target. Target detection is performed in the frequency domain, where targets appear as spectrum peaks which are broadened by the windowing. Both elementspace as well as beamspace signals can be used for target detection. The latter is preferred because of a higher SNR. Several ramps are necessary for a unique estimation of distance and velocity of all targets. The azimuth DOA estimation is also performed in the frequency domain. Up to 3 FFT bins are used for this purpose due to peak broadening. Assuming 4 FMCW ramps, only a fairly small number of 12 snapshots is available for DOA estimation [9].

This project is supported by the German Ministry of Education and Research (BMBF) under contract nr. 16SV2181 (KRAFAS).

One particular restriction in the antenna design is the use of a low-cost small-size dielectric lens (radome) for focussing in elevation instead of a two-dimensional patch array. Due to boundary and reflection effects caused by the radome, each sensor element shows a different direction-dependent gain and phase response depending on its lateral position behind the radome. Fig. 1 shows the sensor responses of all 8 elements for a varying DOA where the phase responses are normalized at $\theta = 0^\circ$. They are calculated from an electromagnetic wave field simulation. Obviously, considerable sensor mismatch exists which will limit the DOA estimation performance if not calibrated.

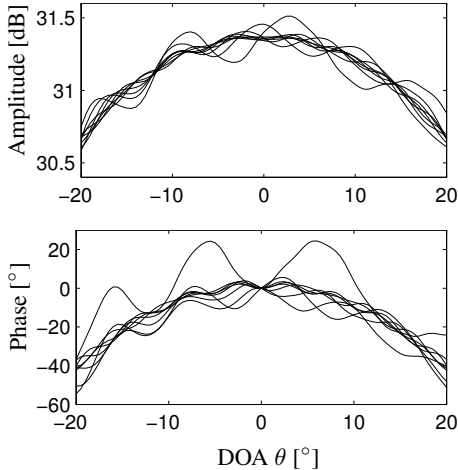


Fig. 1. Direction-dependent sensor mismatch due to boundary and reflection effects of a radome. The phase response is normalized at 0° .

3. SUBSPACE BASED DOA ESTIMATION

We assume p far field narrow band source signals $\mathbf{s}(t)$ impinging on an ULA. The received signal $\mathbf{x}(t)$ can be modeled as

$$\mathbf{x}(t) = \mathbf{A}\mathbf{s}(t) + \mathbf{n}(t) \quad (1)$$

where $\mathbf{A} = [\mathbf{a}(\theta_1) \dots \mathbf{a}(\theta_p)]$ is the steering matrix, $\mathbf{a}(\theta)$ is the steering vector of an ULA for the DOA θ , $\mathbf{s}(t)$ denotes the FMCW radar signals in FFT bins where a target has been detected, and $\mathbf{n}(t)$ describes the sensor noise in the same FFT bins. Here t does not denote the time. It is rather an index of snapshots collected from different FFT bins and different FMCW ramps [9].

Let $\mathbf{R} = \mathbb{E}[\mathbf{x}(t)\mathbf{x}^H(t)]$ be the spatial correlation matrix. Under ideal assumptions of spatially i.i.d. sensor noise as well as uncorrelated source signals and sensor noise, efficient subspace based methods can be applied for high-resolution DOA estimation. Using an eigenvalue decomposition of \mathbf{R} , the obtained noise subspace matrix \mathbf{U}_n with orthonormal columns can be used to calculate, e.g., the MUSIC angular spectrum

$$m(\theta) = \frac{\|\mathbf{a}(\theta)\|^2}{\|\mathbf{U}_n^H \mathbf{a}(\theta)\|^2} \quad (2)$$

whose peaks correspond to target DOAs.

4. CALIBRATION

The performance of high-resolution DOA estimation for automotive radar is limited by a number of factors: number of snapshots, signal to noise ratio (SNR), correlation of the source signals, and sensor errors. In this paper, we study antenna calibration to correct sensor errors.

For a real antenna array, the true steering vector $\tilde{\mathbf{a}}(\theta)$ deviates from the ideal one $\mathbf{a}(\theta)$. The array imperfection can be modeled by

$$\tilde{\mathbf{a}}(\theta) = \mathbf{Q}\mathbf{a}(\theta) \quad (3)$$

where \mathbf{Q} is a square calibration matrix. Gain and phase mismatches between different antenna elements can be modeled by a complex diagonal matrix \mathbf{Q}_{GP} . The coupling between antenna elements is typically described by a full but diagonally dominant matrix $\mathbf{Q} = \mathbf{Q}_C$. Both \mathbf{Q}_{GP} and \mathbf{Q}_C do not depend on DOA. Angle-dependent sensor errors are due to sensor position inaccuracy [8] or a nonideal dielectric lens as in our case. Here $\mathbf{Q} = \mathbf{Q}_L(\theta)$ is a DOA-dependent complex diagonal matrix. The true received signal is then

$$\tilde{\mathbf{x}}(t) = [\tilde{\mathbf{a}}(\theta_1) \dots \tilde{\mathbf{a}}(\theta_k)]\mathbf{s}(t) + \mathbf{n}(t). \quad (4)$$

4.1. Global calibration

In so called global calibration [4, 5, 6, 7], \mathbf{Q} is assumed to be DOA-independent resulting in $\tilde{\mathbf{x}}(t) = \mathbf{Q}\mathbf{A}\mathbf{s}(t) + \mathbf{n}(t)$. The task is to estimate \mathbf{Q} from a number of calibration measurements $\mathbf{x}_j(\theta_j^{\text{cal}})$ ($1 \leq j \leq J$), which are sensor signals for a single emitter at the calibration DOA θ_j^{cal} . For easy notation, let $\mathbf{x}_j = \mathbf{x}(\theta_j^{\text{cal}})$ and $\mathbf{a}_j = \mathbf{a}(\theta_j^{\text{cal}})$. The matrix $\mathbf{X} = [\mathbf{x}_1 \mathbf{x}_2 \dots \mathbf{x}_J]$ contains all calibration measurements, the matrix $\mathbf{A} = [\mathbf{a}_1 \mathbf{a}_2 \dots \mathbf{a}_J]$ the corresponding ideal steering vectors. Below we briefly review some approaches to estimate the global calibration matrix \mathbf{Q} .

Pierre and Kaveh [4] first normalized all measurements \mathbf{x}_j to unit norm. Then they proposed to minimize the sum of squared euclidean distances between $\mathbf{Q}^{-1}\mathbf{x}_j$ and \mathbf{a}_j :

$$\min_{\mathbf{Q}} \|\mathbf{Q}^{-1}\mathbf{X} - \mathbf{A}\|_F^2 = \sum_{j=1}^J \|\mathbf{Q}^{-1}\mathbf{x}_j - \mathbf{a}_j\|^2. \quad (5)$$

See [5] observed that the true steering vectors of a real antenna array may have different lengths. Hence he extended the above approach to

$$\min_{\mathbf{Q}, \mathbf{d}} \|\mathbf{X} \text{diag}(\mathbf{d}) - \mathbf{Q}\mathbf{A}\|_F^2 = \sum_{j=1}^J \|\mathbf{x}_j d_j - \mathbf{Q}\mathbf{a}_j\|^2 \quad (6)$$

where the vector $\mathbf{d} = [d_1 \dots d_J]$ accounts for different complex scalings of the true steering vectors. Both approaches rely on difference based error criteria. The effect is that both direction and length of $\mathbf{Q}\mathbf{a}_j$ should match to those of \mathbf{x}_j or $\mathbf{x}_j d_j$, respectively.

For array processing methods where only the direction and not the length of the steering vector is important (e.g. MUSIC

spectrum), Pense [6] proposed to use an orthogonality criterion. For each calibration measurement \mathbf{x}_j , he found a vector \mathbf{c}_j which is orthogonal to \mathbf{x}_j . The calibration matrix \mathbf{Q} is now determined such that $\mathbf{Q}\mathbf{a}_j$ is as orthogonal to \mathbf{c}_j as possible:

$$\min_{\mathbf{Q}} \sum_{j=1}^J |\mathbf{c}_j^H \mathbf{Q}\mathbf{a}_j|^2 \quad \text{s.t. } \|\mathbf{Q}\|_F^2 = 1. \quad (7)$$

The constraint $\|\mathbf{Q}\|_F^2 = 1$ is necessary to avoid the trivial solution $\mathbf{Q} = \mathbf{0}$. Note that actually each \mathbf{x}_j has an $(M-1)$ -dimensional orthogonal complement and the choice of \mathbf{c}_j is not unique. Kortke [7] proposed a collinearity criterion. The objective is to determine \mathbf{Q} in such a way that $\mathbf{Q}\mathbf{a}_j$ is as parallel to \mathbf{x}_j as possible:

$$\min_{\mathbf{Q}} \sum_{j=1}^J \left(\|\mathbf{x}_j\|^2 \|\mathbf{Q}\mathbf{a}_j\|^2 - |\mathbf{x}_j^H \mathbf{Q}\mathbf{a}_j|^2 \right) \quad \text{s.t. } \|\mathbf{Q}\|_F^2 = 1. \quad (8)$$

These two approaches focus on the direction of $\mathbf{Q}\mathbf{a}_j$ only.

Another issue in estimating the global calibration matrix \mathbf{Q} is the choice of its sparsity. The question, if \mathbf{Q} should be a full, diagonal or a band matrix, depends on the nature of the sensor errors. Another important factor, however, is the number of calibration measurements J in relation to the number of unknown parameters in \mathbf{Q} . For a weak coupling between the sensor elements and a small DOA range of calibration measurements, a tridiagonal \mathbf{Q} might result in a better calibration performance than a full \mathbf{Q} .

4.2. Local calibration

In local calibration, the diagonal calibration matrix $\mathbf{Q}(\theta)$ depends on the DOA of interest. In this case, the previous four approaches can not be applied. For each DOA of interest θ_k^{eval} during evaluation, Lanne et al. [8] proposed to determine $\mathbf{Q}(\theta_k^{\text{eval}})$ by

$$\begin{aligned} \min_{\mathbf{Q}(\theta_k^{\text{eval}})} & \left\| \left(\mathbf{X} - \mathbf{Q}(\theta_k^{\text{eval}})\mathbf{A} \right) \mathbf{W}^{\frac{1}{2}}(\theta_k^{\text{eval}}) \right\|_F^2 \\ & = \sum_{j=1}^J w_j(\theta_k^{\text{eval}}) \left\| \left(\mathbf{x}_j - \mathbf{Q}(\theta_k^{\text{eval}})\mathbf{a}_j \right) \right\|^2 \end{aligned} \quad (9)$$

where $\mathbf{W}(\theta_k^{\text{eval}}) = \text{diag}(w_1(\theta_k^{\text{eval}}), \dots, w_J(\theta_k^{\text{eval}}))$ is a diagonal matrix for weighting the calibration measurements with weightings $w_j(\theta_k^{\text{eval}}) = \exp(-\alpha|\theta_j^{\text{cal}} - \theta_k^{\text{eval}}|)$ and $\alpha > 0$. Its effect is a local exponentially windowed smoothing of the calibration results based on one steering vector.

4.3. How to use the calibration matrix

Once we have estimated the global or local calibration matrix $\hat{\mathbf{Q}}$, there are two different ways to use it. The first approach is to process the received sensor vector $\tilde{\mathbf{x}}(t) = \mathbf{Q}\mathbf{A}\mathbf{s}(t) + \mathbf{n}(t)$ as usual like the estimation of the noise subspace matrix $\hat{\mathbf{U}}_n$ from the correlation matrix of $\tilde{\mathbf{x}}(t)$. We use the approximated true steering vector $\hat{\mathbf{Q}}(\theta)\mathbf{a}(\theta)$ instead of the ideal one $\mathbf{a}(\theta)$ in the MUSIC spectrum

$$m(\theta) = \frac{\|\hat{\mathbf{Q}}(\theta)\mathbf{a}(\theta)\|^2}{\|\hat{\mathbf{U}}_n^H \hat{\mathbf{Q}}(\theta)\mathbf{a}(\theta)\|^2} \quad (10)$$

and maximize it over θ . This approach is applicable to both global and local calibration. In global calibration, $\hat{\mathbf{Q}}(\theta)$ is fixed and independent of θ . In local calibration, $\hat{\mathbf{Q}}(\theta) = \hat{\mathbf{Q}}(\theta_k^{\text{eval}})$ if $\theta = \theta_k^{\text{eval}}$, or a linear interpolation of the amplitudes and phases of the diagonal elements of $\hat{\mathbf{Q}}(\theta_k^{\text{eval}})$ otherwise. The main advantage of this approach is that the noise $\mathbf{n}(t)$ is still spatially white. This simplifies the subspace discrimination and order estimation. The main drawback is that decorrelation algorithms like spatial smoothing can not be applied since we lose the ULA property due to $\hat{\mathbf{Q}}(\theta)\mathbf{a}(\theta)$ even if the ideal array is an ULA.

The second approach is to restore the ideal steering vector by using the inverse calibration matrix

$$\mathbf{x}_{\text{cor}}(t) = \hat{\mathbf{Q}}^{-1}\tilde{\mathbf{x}}(t) = \mathbf{A}\mathbf{s}(t) + \hat{\mathbf{Q}}^{-1}\mathbf{n}(t). \quad (11)$$

Algebraic methods for DOA estimation like rooting methods or ESPRIT can then be applied to $\mathbf{x}_{\text{cor}}(t)$. Also correlated signals can be dealt with decorrelation algorithms. One drawback of this approach is that the transformed noise $\hat{\mathbf{Q}}^{-1}\mathbf{n}(t)$ is in general not spatially white, but with a known correlation matrix. Another disadvantage is that this approach is not applicable to local calibration. If $\tilde{\mathbf{x}}(t)$ contains a mixture of incoming signals from different DOAs, which local calibration matrix $\hat{\mathbf{Q}}(\theta)$ should be used in (11)?

In the following, we will use the first approach, i.e. the MUSIC spectrum (10), for DOA estimation for a fair comparison between global and local calibration.

5. SIMULATIONS AND RESULTS

Since this radar sensor is still under development, we use MATLAB to simulate both calibration measurements and calibration as well as DOA estimation.

5.1. Calibration

The sensor errors of the dielectric lens, as depicted in Fig. 1, are taken from electromagnetic field simulations. Coupling between elements is simulated using a log-normally distributed random process for the amplitudes of the coupling matrix \mathbf{Q}_C , with standard deviation $\sigma_C = 2\text{dB}$ and mean $\mu_{12} = -20\text{dB}$ for coupling between direct neighbours and $\mu_{13} = -30\text{dB}$ for coupling to other elements, respectively. The phase of all coupling elements is uniformly distributed between 0 and 2π . Gain mismatch is simulated using a zero-mean log-normally distributed random process with standard deviation $\sigma_G = 1.0\text{dB}$. Phase mismatch is simulated with a uniformly distributed random process in the range $[-20^\circ \ 20^\circ]$. The antenna is an 8 element ULA with $d = \lambda$. We always use 12 snapshots only in both calibration and DOA estimation. The simulated calibration measurements are taken in the DOA range $-\theta_{\text{max}}^{\text{cal}} = \theta_1^{\text{cal}} \leq \theta_j^{\text{cal}} \leq \theta_j^{\text{cal}} = \theta_{\text{max}}^{\text{cal}}$ with the DOA step $\Delta\theta^{\text{cal}} = \theta_j^{\text{cal}} - \theta_{j-1}^{\text{cal}}$. In order to simulate the DOA uncertainty when placing the transmitter in calibration measurements, the true calibration DOAs θ_j^{cal} are perturbed by adding a zero-mean Gaussian random angle θ_{rand} with standard deviation $\sigma_{\theta^{\text{cal}}}$. If the realization of θ_{rand} is larger than $0.9\Delta\theta^{\text{cal}}$, it is dropped and

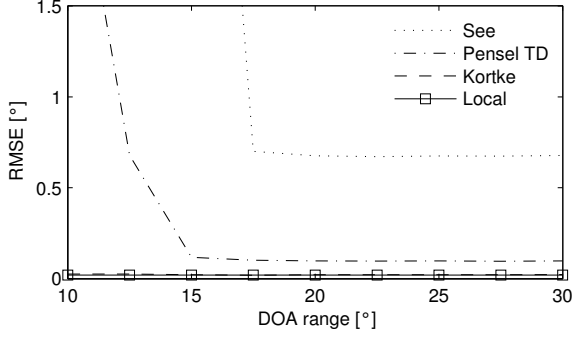


Fig. 2. RMSE vs. DOA range $\theta_{\max}^{\text{cal}}$ of calibration

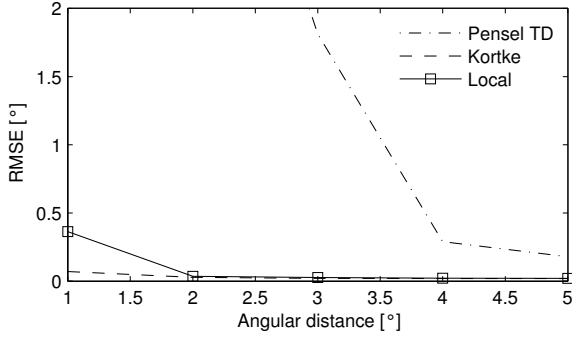


Fig. 3. RMSE vs. angular distance $\Delta\theta$ of 2 targets

new realization is generated. The SNR used is 50dB (corner reflector in close proximity). The calibration measurement vectors \mathbf{x}_j are derived from eigenanalysis of the simulated received signal as in [4]. Once the calibration measurements \mathbf{X} are generated, different calibration algorithms are used to estimate the calibration matrix \mathbf{Q} .

5.2. DOA estimation

We use the MUSIC spectrum (10) for DOA estimation. There is either one signal target or two uncorrelated targets with equal power. The number of targets is assumed to be known. The SNR for each target is 40dB, so DOA estimation errors are mainly due to imperfect calibration and a limited number of 12 snapshots. In case of one target, the DOA of the target is varied between $\pm 8^\circ$ in steps of roughly 0.5° . For two targets, one of the DOAs is varied in the same range, and the second DOA is kept at a fixed angular distance $\Delta\theta = \theta_2 - \theta_1$. The MUSIC maximum search is performed in the range of $\pm 15^\circ$ in steps of 0.1° , the DOA estimation is refined using peak interpolation for the highest peaks. From all DOA estimates of 250 trials and all target DOAs, we calculate the root mean squared error (RMSE).

5.3. Accuracy Results

In the following, we present some simulation results to compare the algorithms by See [5], Pensel [6], and Kortke [7] for global calibration with that by Lanne [8] for local calibration.

In Fig. 2, we plot the RMSE of DOA estimation versus the DOA range $\theta_{\max}^{\text{cal}}$ of calibration measurement with a fixed DOA step of $\Delta\theta^{\text{cal}} = 1^\circ$. For our application, a long range radar, this study is of particular importance since the transmitting antenna is focused only on a small angular field of view. This results in a small DOA range available for calibration measurement as well. Without any calibration, the RMSE value is roughly 0.33° . For the Pensel algorithm, we used a tridiagonal (TD) calibration matrix \mathbf{Q} as we observed numerical difficulties when using a full matrix \mathbf{Q} . The local calibration used a DOA step of $\Delta\theta_k^{\text{eval}} = 1^\circ$ and $\alpha = 2$ during evaluation of $\mathbf{Q}(\theta_k^{\text{eval}})$. The calibration measurement is assumed to be perfect ($\sigma_{\theta^{\text{cal}}} = 0$). As we see from Fig. 2, the performance of the algorithm by See (and by Pierre & Kaveh) is pretty bad. The algorithm by Pensel achieves a considerable improvement, in particular for $\theta_{\max}^{\text{cal}} \geq 15^\circ$. The best result is achieved by the Kortke algorithm and the local calibration. Their RMSE value in this experiment is roughly 0.02° .

In Fig. 3, the RMSE of two targets is shown for a varying target angular distance. In this experiment with $\theta_{\max}^{\text{cal}} = 20^\circ$, we were only able to resolve the close targets with the algorithms by Pensel, Kortke, and Lanne. The Kortke algorithm outperforms the others. This is due to the collinearity criterion which seems to be best suitable for MUSIC DOA estimation.

To simulate real calibration measurements, the standard deviation of the calibration DOA $\sigma_{\theta^{\text{cal}}}$ is now varied between 0° and 0.1° . The latter is equivalent to a standard deviation of about 10mm for a corner reflector in 6m distance. Fig. 4 shows the simulation results. Obviously, the algorithm by See is also very sensitive to the calibration DOA errors. The algorithm by Pensel and the local calibration are quite robust. Their RMSE values are well below the required DOA accuracy of 0.4° . The Kortke algorithm satisfies this requirement only if $\sigma_{\theta^{\text{cal}}} < 0.08^\circ$.

As we see from Fig. 5, the Pensel algorithm is sensitive to the DOA step $\Delta\theta^{\text{cal}}$. The Kortke algorithm, however, is very robust against $\Delta\theta^{\text{cal}}$. At least in the range $0^\circ \leq \Delta\theta^{\text{cal}} \leq 3^\circ$, the RMSE of the Kortke algorithm remains almost constant around 0.02° .

For the local calibration, there is an interesting observation. If the calibration DOA grid θ_j^{cal} and evaluation DOA grid θ_k^{eval} coincide, e.g. $\Delta\theta^{\text{cal}} = \Delta\theta^{\text{eval}} = 1^\circ, 2^\circ$ or 3° , we achieve the best performance. In this case, the local calibration returns approximated steering vectors $\hat{\mathbf{Q}}\mathbf{a}_j$ which are almost collinear to the cor-

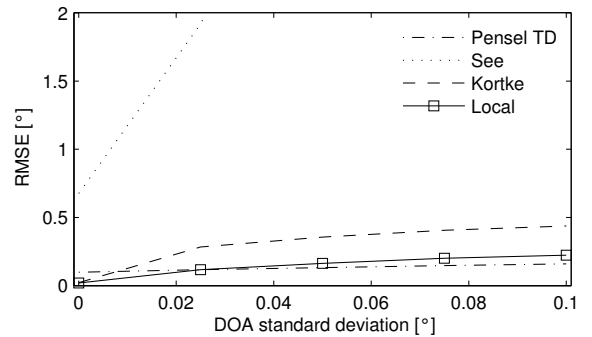


Fig. 4. RMSE vs. DOA standard deviation $\sigma_{\theta^{\text{cal}}}$

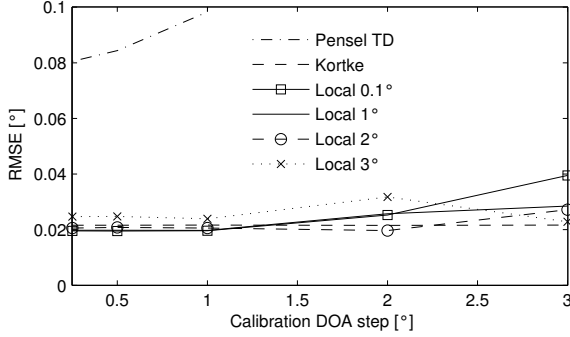


Fig. 5. RMSE vs. calibration DOA step $\Delta\theta^{\text{cal}}$

responding true steering vector \mathbf{x}_j . This is not the case if θ_k^{eval} does not coincide with any θ_j^{cal} . In Fig. 5 with $\Delta\theta^{\text{cal}} = 3^\circ$, the performance of using the same grid $\Delta\theta^{\text{eval}} = 3^\circ$ for evaluation is better than using a finer evaluation DOA grid with $\Delta\theta^{\text{eval}} = 2^\circ, 1^\circ$, or even 0.1° .

5.4. Implementation cost

In this subsection, we briefly compare the global and local calibration with respect to the implementation cost. The estimation of the global or local calibration matrix \mathbf{Q} from the calibration measurements is typically done offline. For the global calibration, we need to estimate and store a fixed calibration matrix \mathbf{Q} . In the case of local calibration, we need to estimate and store many different diagonal calibration matrices $\mathbf{Q}(\theta_k^{\text{eval}})$ at an evaluation DOA grid θ_k^{eval} . Clearly, the memory requirement of local calibration is higher if the number of evaluation DOAs is larger than the number of antenna elements.

For the calculation of the MUSIC spectrum (10), we have to take into account that $\hat{\mathbf{Q}}$ for the global calibration is in general a full matrix. In contrast, each $\hat{\mathbf{Q}}(\theta)$ for the local calibration is diagonal resulting in a low computational complexity for the calculation of $\hat{\mathbf{Q}}\mathbf{a}$. The need of interpolating $\hat{\mathbf{Q}}(\theta)$ if $\theta \neq \theta_k^{\text{eval}}$ can be reduced if we choose a fine evaluation DOA grid at the expense of a higher memory requirement. If we choose to save computational effort by storing $\tilde{\mathbf{a}}(\theta) = \hat{\mathbf{Q}}(\theta)\mathbf{a}(\theta)$ in a fine grid, the computational effort for calculating $\hat{\mathbf{Q}}\mathbf{a}$ is shifted to offline calibration, and the memory and computational effort is the same for both global and local calibration.

6. CONCLUSIONS

In this paper, we studied different approaches for global and local calibration of an automotive radar antenna array. Both algorithms to estimate the calibration matrix and strategies to use it in high-resolution DOA estimation were discussed. In an experiment to correct DOA-dependent sensor errors caused by a dielectric lens in addition to gain/phase mismatch and coupling between the elements, the local calibration shows its superior performance. Surprisingly, also the global calibration technique proposed by Kortke achieves a comparable performance except for

a slightly higher sensitivity with respect to the DOA accuracy of calibration measurements. In contrast, the least squares based approaches by Pierre and Kaveh as well as See fail in our experiments. The reason is that the collinearity between the true and approximated steering vector is a better error criterion than their distance for DOA estimators which rely on the orthogonality between the signal and noise subspace.

The authors would like to thank all partners of the KRAFAS consortium, especially Peter Wenig from University of Erlangen for dielectric lens simulations.

7. REFERENCES

- [1] Martin Schneider, “KRAFAS - Innovationen in der Mikrosystemtechnik und der Hochfrequenz-Mikroelektronik für kostenoptimierte Radarsensoren im Automotive-Bereich,” in *VDE Kongress*, Aachen, Germany, 2006, pp. 275–282.
- [2] Merrill I. Skolnik, *Introduction to Radar Systems*, McGraw-Hill, 3 edition, 2001.
- [3] Hamid Krim and Mats Viberg, “Two decades of array signal processing research,” *IEEE Signal Processing Magazine*, vol. 13, no. 4, pp. 67–94, July 1996.
- [4] J. Pierre and M. Kaveh, “Experimental performance of calibration and direction-finding algorithms,” in *Proc. IEEE Conference on Acoustics, Speech, and Signal Processing (ICASSP)*, 1991, pp. 1365–1368.
- [5] C. M. S. See, “Sensor array calibration in the presence of mutual coupling and unknown sensor gains and phases,” *Electronics Letters*, vol. 30, no. 5, pp. 373–374, Mar. 1994.
- [6] K. Pensel, H. Aroudaki, and J.A. Nossek, “Calibration of smart antennas in a GSM network,” in *Proc. Signal Processing Advances in Wireless Communications (SPAWC)*, 1999.
- [7] Andreas Kortke, “A new calibration algorithm for smart antenna arrays,” in *Proc. Vehicular Technology Conference*, Apr. 2003.
- [8] Maria Lanne, Astrid Lundgren, and Mats Viberg, “Calibrating an array with scan dependent errors using a sparse grid,” in *Proc. Asilomar Conference on Signals, Systems and Computers (ACSSC)*, 2006, pp. 2242–2246.
- [9] Michael Schoor and Bin Yang, “High-resolution angle estimation for an automotive FMCW radar sensor,” in *Proc. Intern. Radar Symposium (IRS)*, Cologne, Germany, Sept. 2007.